

Instantaneous Crossflow Topology on a Delta Wing in Presence of Vortex Breakdown

K. M. Cipolla* and D. Rockwell†
Lehigh University, Bethlehem, Pennsylvania 18015

The crossflow structure of the leading-edge vortices on a delta wing is investigated via particle image velocimetry. The transformation of the streamline topology as the vortex breakdown position moves up- or downstream of its nominal value is characterized by comparing instantaneous images. While the streamline patterns are distinctly different depending on the location of vortex breakdown relative to the field of view, contours of constant vorticity do not exhibit such distinctions. Several classes of instantaneous streamline topology can exist in the crossflow plane. These topologies, which involve various combinations of limit cycles and foci, indicate the importance of considering the instantaneous nature of both the vorticity contours and streamlines when describing the flow physics.

Nomenclature

c_o = centerline chord
 d_f = interrogation window size
 t = time
 U = freestream velocity
 x_L = location of laser sheet
 x_{vb} = location of vortex breakdown, measured along wing centerline from apex
 Δl = interrogation step size
 ϕ = roll angle
 ω = out-of-plane vorticity

Introduction

THE flow past a delta wing is characterized by the existence of vortices that separate from its leading edges. The structure of these vortices has been the focus of considerable investigation via experimental and numerical studies. One method that has emerged to interpret the results of such studies is the use of topological concepts to describe the two-dimensional sectional streamline patterns. The applicability of this approach has been discussed by Tobak and Peake,¹ Perry and Chong,² and Visbal.³ For flow past a stationary delta wing at low angles of attack, the leading-edge vortex has been represented traditionally as a stable, inwardly spiraling focus.⁴ More recent works involving delta wings at high angles of attack that undergo pitching motion have shown that this description is not universally valid, and that several distinct topologies may exist in a crossflow plane cutting through the leading-edge vortex.^{5,6} However, the structure of the flow in the region downstream of vortex breakdown, where stall occurs, is much more complex and, therefore is less understood. A topological description of the flow structure as the vortex breakdown position varies relative to the plane of view is provided by Visbal and Gordnier⁶ in their numerical study of a pitching delta wing.

The behavior of the leading-edge vortices has been described, in most experimental studies, in terms of the variation of the location of vortex breakdown. At the onset of break-

down, there is a sudden expansion of the cross-sectional area of the core of the vortex. Although this is a dominant, easily identifiable feature of the flow past a delta wing, it does not provide quantitative information about the flow pattern. Various studies describe the aerodynamic reactions of a delta wing during a roll maneuver.^{7–10} Several studies, including that of Jenkins et al.,¹¹ have developed nonlinear models for the aerodynamic loading of delta wings based on the results of these experimental investigations. However, to date, an adequate quantitative description of the alterations of the leading-edge vortex structure, with variations in roll angle and the corresponding variations in vortex breakdown location, has not been available. By obtaining the instantaneous patterns of vorticity and streamlines in crossflow planes via particle image velocimetry (PIV) and examining how these patterns vary as the roll angle changes, the present investigation intends to provide a basis for understanding the fluid dynamics behind the aerodynamic reactions observed in previous studies.

To this end, the structure of the leading-edge vortices on a delta wing, both upstream and downstream of vortex breakdown, is characterized using high-image density PIV. Instantaneous velocity fields, contours of constant vorticity, and sectional streamline patterns are obtained in a crossflow plane oriented perpendicular to the centerline of the wing when the wing is fixed at various roll angles. It is demonstrated that monitoring topological features of the instantaneous streamline patterns is an effective method for tracking physical bifurcations in the flow, as the vortex breakdown position varies relative to the plane of view. Furthermore, the instantaneous images can be compared to an image obtained by averaging a number of such images, which preserves the general form of the streamline topology.

Experimental System and Techniques

Experiments were performed in a large, open-surface water channel, with a test section approximately 1 m wide by 0.5 m deep. The flow speed was 17.8 cm/s, corresponding to a Reynolds number based on the wing centerline chord of 32,400. The delta wing used in the experiment had a sweep angle of 65 deg and a $c_o = 20.3$ cm (Fig. 1). The wing was mounted on a sting $3c_o$ in length at an angle of attack $\alpha = 30$ deg. Details of the experimental setup, including computer-controlled movement of the wing and the components of the image acquisition system, are given in Refs. 12 and 13. The zero-roll-angle condition is established as the position where the opposite leading-edge vortex breakdown locations are symmetric. Dye injected at the apex of the delta wing (Fig. 1)

Received Sept. 9, 1996; revision received Sept. 3, 1997; accepted for publication Sept. 4, 1997. Copyright © 1998 by K. M. Cipolla and D. Rockwell. Published by the American Institute of Aeronautics and Astronautics, Inc., with permission.

*Graduate Research Assistant, Department of Mechanical Engineering; currently Mechanical Engineer, U.S. Naval Undersea Warfare Center, Newport, RI 02840.

†Paul B. Reinhold Professor, Department of Mechanical Engineering. Member AIAA.

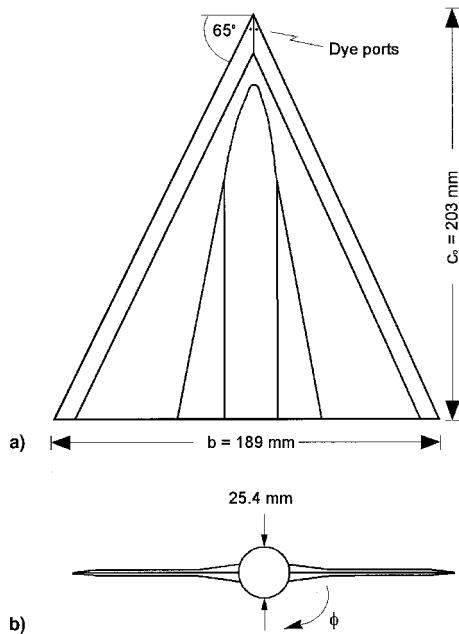


Fig. 1 Delta wing geometry: a) plan view and b) end view.

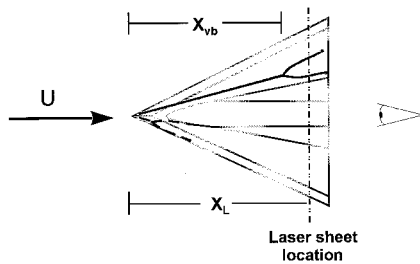


Fig. 2 Definition of locations of laser sheet and vortex breakdown.

marks the leading-edge vortex and enables tracking of the vortex breakdown position, which, even for the case of the stationary wing, was observed to exhibit substantial chordwise fluctuations, in accord with the observations of Gursul and Yang.¹⁴

The instantaneous velocity fields over an entire plane of the flow were obtained via scanning PIV.¹⁵ A multi-(72)-faceted mirror rotates at 8.7 Hz to produce a 1-mm-thick laser sheet at an effective scanning rate of 626 Hz. The images obtained as 35-mm film negatives were interrogated by a program that uses a single-frame, cross-correlation method involving the application of two successive fast Fourier transforms.¹⁶ A typical $d_t \times d_t$ of 0.72×0.72 mm was used with a 50% overlap, thereby satisfying the Nyquist criterion, i.e., Δt did not exceed $0.5d_t$. The resulting grid size on the film was 0.36×0.36 mm, corresponding to 2.25×2.25 mm in the physical plane, with the magnification of the lens equal to 0.17.

The laser sheet was oriented perpendicular to the centerline of the delta wing at $x_L = 0.90 c_0$ downstream of the apex (Fig. 2), acquired with a 35-mm camera at 20-s intervals after the flow had reached a quasisteady state.

Results and Discussion

In this investigation, inherent instabilities in the flow will be revealed by studying variations in the instantaneous flow patterns for a stationary delta wing over a range of ϕ . Consideration of images taken in planes downstream of vortex breakdown will provide the first detailed insight into the flow structure in the stall region. These patterns can be compared to those obtained when the delta wing is at an extreme value of roll angle, for which the vortex breakdown location is

downstream of the trailing edge. Topology concepts will be especially useful for characterizing variations in the flow structure for each of these cases. The transformation of the flow structure as the vortex breakdown location moves upstream will be interpreted via topological features in the instantaneous streamlines.

In all plots of vorticity and streamlines in crossflow planes, the flow is out of the page, such that the right-hand side of each image corresponds to the starboard side of the delta wing and the left-hand side corresponds to the port side. Positive vorticity (counterclockwise) is indicated by solid curves, and negative vorticity is indicated by dashed curves. The values of ω_{\min} and $\Delta\omega$ are stated in each caption. The cross section of the delta wing is shown in gray in each image. Arrows superimposed on the streamlines illustrate the local flow direction. The location of vortex breakdown relative to x_L , normalized by c_0 , i.e., $(x_{vb} - x_L)/c_0$, is specified adjacent to each image or in the figure caption.

Flow Structure of Leading-Edge Vortices: Breakdown Region

Observation at a Location Immediately Downstream of the Onset of Vortex Breakdown

Figure 3 shows examples of instantaneous sectional streamlines (left column) and the corresponding patterns of out-of-plane vorticity (right column) acquired in a crossflow plane immediately downstream of vortex breakdown. For this set of data, the delta wing is at $\phi = -10$ deg. The images are acquired in a crossflow plane, located at 90% chord, as described in the Experimental System and Techniques section and as shown schematically in Fig. 2. Prior to acquiring images in 20-s intervals, the leading-edge vortices were allowed to reach an equilibrium state, monitored via dye visualization. In the complete set of data, x_{vb}/c_0 ranges from 0.54 to 0.69 [corresponding to $(x_{vb} - x_L)/c_0 = -0.36$ to -0.21 , as indicated below

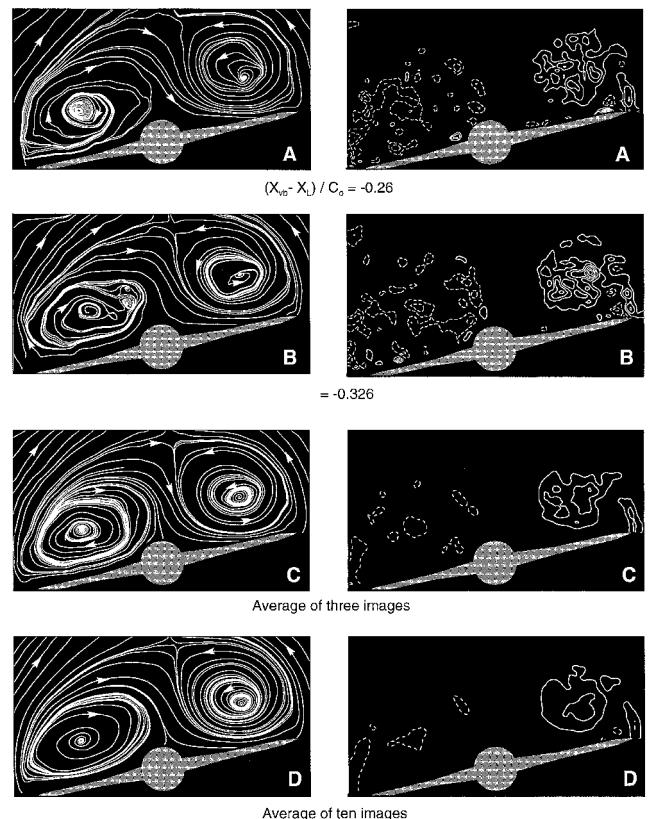


Fig. 3 Streamline patterns and vorticity fields in the breakdown region of a stationary delta wing. $\phi = -10$ deg, minimum and incremental contour levels are $\omega_{\min} = \pm 10 \text{ s}^{-1}$ and $\Delta\omega = 10 \text{ s}^{-1}$. Relative locations of the onset of vortex breakdown given are for the starboard side.

each set of images] on the starboard side and from 0 to 0.5 on the port side, and therefore occurs upstream of the field of view (FOV) in all of the images of Fig. 3. These values are consistent with the dye visualization results presented in Ref. 13.

Although x_{vb} occurs upstream of the plane of the laser sheet for each image of Fig. 3, inherent, relatively small fluctuations of x_{vb} induce variations in the corresponding streamline topologies. The most common topology seen in the instantaneous images of this stalled flow is an unstable limit cycle, characterized by an outwardly spiraling streamline surrounding an inwardly spiraling streamline, with a closed trajectory in between. This crossflow topology, observed for both of the leading-edge vortices of image A, is consistent with the numerical results of Visbal and Gordnier⁶ for chordwise locations downstream of vortex breakdown. In image B, the dominant topologies again are in the form of unstable limit cycles, but the structure exhibits small-scale irregularities near the vortex core on the port side.

Further inspection of images A and B reveals additional topological features. A saddle point, indicating a stagnation point in the two-dimensional flowfield, consistently exists at the upper edge of each image. Note that this saddle point indicates a location where the in-plane velocity components have zero value, not a true three-dimensional stagnation point. The location of this saddle point is shifted toward the starboard side of the wing because of the nonzero roll angle. Also, in images A and B, a coalescence of streamlines occurs just above the port wing surface. This feature is known as an open bifurcation line, associated with the existence of an out-of-plane stream surface.¹⁷ Any flow asymmetry will cause this surface to roll up, producing a vorticity vector parallel to the bifurcation line. In images A and B of Fig. 3, the flow beneath the primary vortex is confined by the wing and flows along the surface. The coalescence of the streamlines implies a vorticity vector parallel to the wing, or in the spanwise direction. Finally, in each of the instantaneous images shown, the streamline that separates from the leading edge is not entrained into the vortical flow, a feature observed in computed instantaneous crossflow topologies downstream of vortex breakdown.⁶ Rather, the streamline patterns clearly show that flow originating on the port side traverses to the starboard side of the wing. This entrainment of flow from one side of the wing to the other suggests the existence of coupling between the opposite leading-edge vortices.

The contours of constant vorticity displayed in the right-hand column of Fig. 3 show a more coherent pattern on the starboard side of the wing, where vortex breakdown occurs closer to the plane of the laser sheet than on the port side. The highly dispersed pattern on the port side indicates a region of severe stall. For both the starboard and port sides, however, the layer of vorticity emanating from the leading edges exhibits the features of a separated shear layer with small-scale concentrations of vorticity. This vorticity eventually rolls around itself to form the primary vortex structure.

It is interesting to note instances for which alterations in the vorticity pattern are not accompanied by corresponding changes in the sectional streamlines, and vice versa. The instantaneous distributions of vorticity on the port side of the wing have relatively low levels and are not at all repeatable in images A and B. Nevertheless, the corresponding instantaneous topologies of the streamline pattern take on recognizable forms. A relatively small-diameter unstable limit cycle is detectable in image A, whereas a substantially larger-scale limit cycle, also unstable, is evident in image B. Also, these streamline topologies reveal small-scale structures that exist in the flow but cannot be discerned readily by inspection of the patterns of constant vorticity contours. On the starboard side of the wing, the vortex in image B has a larger value of maximum vorticity than that in image A. Although this is evident in the more coherent vorticity pattern and the closely spaced vorticity

contours, the streamline topology is relatively unaffected. That is, the streamline topology on the starboard side of the wing in both images A and B takes the fundamental form of an unstable limit cycle. Also, comparing the contours of vorticity would not reveal the existence of different rates of stretching along the axes of the starboard vortices, shown by variations in the degree of spiraling in the streamline patterns in Fig. 3. The preceding observations demonstrate that consideration of either streamline or vorticity patterns alone does not provide a complete picture of the flow structure.

To demonstrate that averaging of the instantaneous flow patterns preserves the general form of the flow topology, an average of 3, then 10, instantaneous images is shown in patterns C and D of Fig. 3. Note, first of all, that the averaging process substantially reduces the peak level of instantaneous vorticity and, furthermore, decreases the number of small-scale, randomly located concentrations of vorticity. For the nonbroken-down vortex on the starboard side of the wing, the general form of the large-scale organized vorticity concentration is retained, but the small-scale concentrations are effectively smoothed out. For the average of 10 images, the concentric vorticity contours approach that of the classical leading-edge vortex. Despite this substantial smoothing of the instantaneous vorticity, the averages of 3 and 10 images show that the general form of the unstable limit cycle is preserved in the streamline topology. That is, the unstable limit cycle topology has a characteristic diameter of the same order as that in images A and B. However, the small-scale distortions of the streamline patterns, evident in the instantaneous images of A and B, are not discernible in the averaged images.

Observation at a Location Well Downstream of the Onset of Vortex Breakdown

Figure 4 shows three selected images for which the crossflow plane, located at 90% chord, lies well downstream of the location of vortex breakdown, i.e., in the stall region. In this case, the delta wing is at $\phi = 0$ deg and instantaneous images are acquired in 20-s intervals, after the leading-edge vortices were allowed to reach an equilibrium state. Again, the FOV is oriented such that the flow is out of the page. In this case, $(x_{vb} - x_L)/c_0$ (Fig. 2) is approximately -0.66 on both the port and starboard sides of the wing, well upstream of the laser sheet.

At $\phi = 0$ deg, it is possible to generate instantaneous locations of vortex breakdown that occur at approximately the same location on either side of the wing. Two instantaneous states, $t = t_1$ and t_2 , are shown for this case. The contours of constant vorticity on both the port and starboard sides of the wing show small-scale concentrations of vorticity that vary in spatial position, not only between opposite sides of the wing, but also from one instantaneous image to the next. Despite these nondeterministic patterns of vorticity, the corresponding streamline topologies indicate identifiable forms. At $t = t_1$, the instantaneous topology on both the port and starboard sides has the form of an unstable (outwardly spiraling) focus, in the absence of a limit cycle. On the other hand, at $t = t_2$, well-defined, unstable limit cycles are evident on both the port and starboard sides. (Note that this topological form matches those presented in Fig. 3, when the delta wing is at $\phi = -10$ deg.) This comparison at $t = t_1$ and t_2 indicates that fundamentally different topologies can be generated at different instants well within the region of vortex breakdown or stall, even if the instantaneous location of the onset of vortex breakdown, as specified by qualitative visualization, is the same at two different instants. As observed in Fig. 3, the streamlines emanating from the leading edges are not entrained into the spiral pattern for this stalled flow, and a saddle point exists at the upper edge of each image. This saddle point is approximately centered over the span because the wing is at a zero roll angle.

To demonstrate the predominant topology, 10 images were ensemble-averaged; they are shown at the bottom of Fig. 4. The overall form of this topology is an unstable focus, though

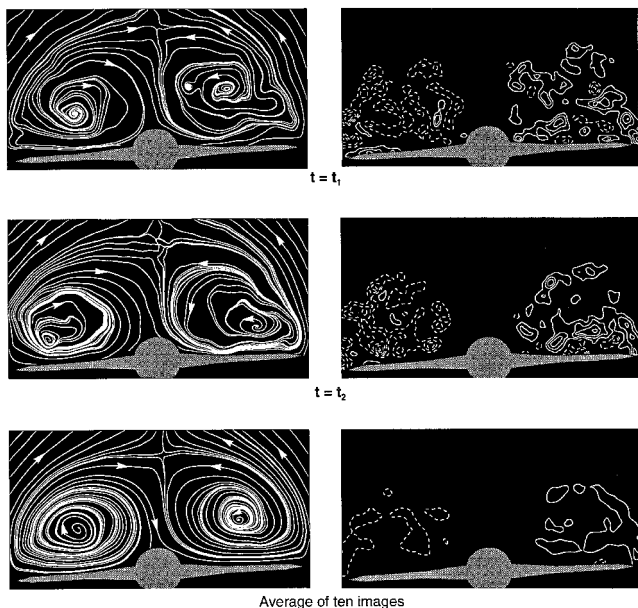


Fig. 4 Streamline patterns and vorticity fields in the breakdown region of a stationary delta wing. $\phi = 0$ deg, $(x_{vb} - x_L)/c_0 \cong -0.66$, $\omega_{\min} = \pm 10 \text{ s}^{-1}$, and $\Delta\omega = 10 \text{ s}^{-1}$.

a very small-scale limit cycle is evident on the starboard side of the wing. Comparison of this averaged topology with the instantaneous topology at $t = t_2$ shows dramatic differences. It is evident that the instantaneous topology at this location well downstream of vortex breakdown, i.e., in the region of substantial stall, cannot be used to deduce the averaged topology, or vice versa. Moreover, upon averaging, maximum levels of the contours of constant vorticity are decreased by 50%, and small-scale structures are eliminated.

Flow Structure of Leading-Edge Vortices: Upstream of Vortex Breakdown

The flow topology in crossflow planes upstream of vortex breakdown is investigated by considering a case for which the delta wing is fixed at $\phi = -20$ deg. At this extreme value of ϕ , large, instantaneous excursions of vortex breakdown occur, with the location of vortex breakdown occurring at or downstream of the trailing edge of the delta wing on the starboard side, and at the apex on the port side. Figure 5 shows the sectional streamline patterns (left column) and the contours of constant vorticity (right column) for the starboard vortex only, in a plane located at 90% chord. The plots are two selected instantaneous images (A and B) and the ensemble-average of 12 instantaneous images (C) from a series of such images taken at 20-s intervals after the flow has reached equilibrium. The relative location of the onset of vortex breakdown is given below each instantaneous image A and B. As for previous figures, these variations of the onset of vortex breakdown are an inherent, self-excited characteristic of the flow, even at this extreme value of roll angle.

Considering the instantaneous contours of vorticity, they are observed to have a remarkably similar form, despite the substantial difference in location of vortex breakdown. They are characteristic of the prebreakdown state of a leading-edge vortex, i.e., highly concentrated vorticity at the center, with only minor, randomly located small-scale concentrations of vorticity. In each image, the shear layer is seen to feed into the primary vortex. The fact that these similar vorticity concentrations cannot be employed to deduce the instantaneous streamline topology is evident from the fundamentally different topologies of images A and B, corresponding, respectively, to an unstable focus and a stable limit cycle.

In general, the streamline topology of images A and B (Fig. 5) agree with numerical results⁶ for crossflow planes far up-

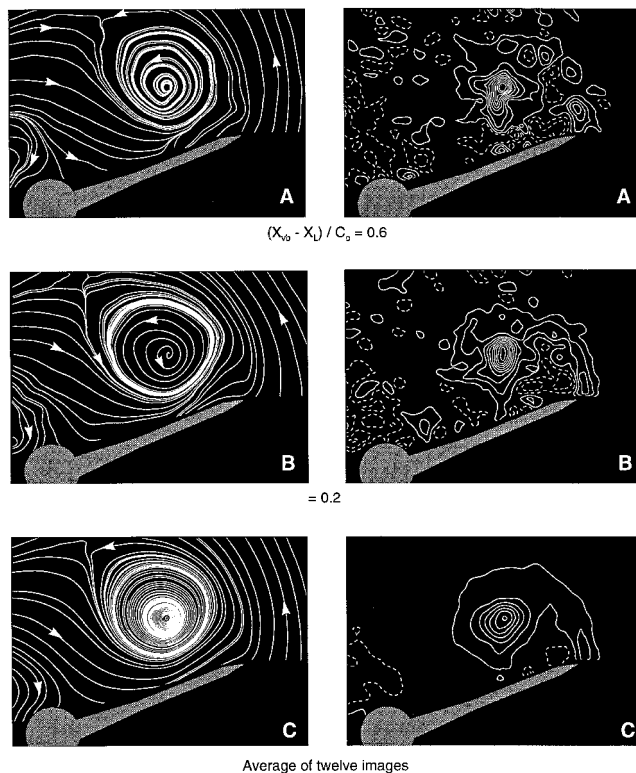


Fig. 5 Instantaneous streamline patterns and vorticity fields in a plane upstream of breakdown for a stationary delta wing. $\phi = -20$ deg, $\omega_{\min} = \pm 5 \text{ s}^{-1}$, and $\Delta\omega = 10 \text{ s}^{-1}$.

stream and just upstream of vortex breakdown, respectively. The stable (inwardly spiraling) focus seen in the streamline pattern of image A represents a case for which the vortex breakdown location is well downstream of the FOV. This topology also is consistent with that observed by Vorobieff¹⁸ for a crossflow plane upstream of the onset of vortex breakdown, and is associated with stretching along the vortex axis. A slight upstream movement of the vortex breakdown location causes a transformation of the topology to a stable limit cycle, as shown in image B. (A stable limit cycle is characterized by an inwardly spiraling streamline surrounding an outwardly spiraling streamline, with a closed trajectory in between.) The unstable focus in the vortex core region is associated with compression along the axis of the vortex⁶ and is an indication of impending vortex breakdown.¹⁸

To demonstrate the average of these fundamentally different topologies, 12 images were randomly averaged and are represented in row C of Fig. 5. This sample included images for which the location of vortex breakdown is at values as extreme as the two preceding images, A and B. We note that the average distribution of vorticity closely resembles that of the classical, time-averaged representation of a leading-edge vortex with a feeding sheet. Nearly all of the small-scale vorticity concentrations have been removed. The corresponding streamline topology shows two clearly identifiable limit cycles nested within each other, distinct from either of the instantaneous topologies of A and B. The numerical calculations of Visbal and Gordnier⁶ also revealed nested limit cycles in the crossflow streamline topology of a primary leading-edge vortex upstream of breakdown.

Taking an overview of the observations of Fig. 5, the overall form of the patterns of vorticity is similar in images A through C, with small-scale distortions from the instantaneous versions of A and B. This consistency, however, provides no indication of the fundamentally different streamline topologies. Comparison of the vorticity patterns in Fig. 5 with those in Figs. 3 and 4 illustrates that the location of maximum vorticity is

closer to the wing surface when the crossflow plane is taken at a position upstream of vortex breakdown. Also, the spatial extent of the vorticity is smaller, i.e., the overall leading-edge vortex structure is more coherent than in the breakdown region.

The majority of the crossflow topologies observed upstream of the location of the onset of leading-edge vortex breakdown involve tight spiral patterns with very closely spaced streamlines. To confirm that the spatial resolution of the data was sufficient to resolve these streamline patterns, an instantaneous image was passed through several different filters. A comparison of the results is given in Cipolla.¹³ Overall, very little modification of the streamline pattern is generated by this increased filtering. Because the main features of the original image were found to remain even after the highest degree of smoothing or filtering, it was concluded that the rapid rate of spiraling in the streamline topologies is genuine and is not an artifact of insufficient resolution.

Flow Structure of Leading-Edge Vortices: Immediate Vicinity of Vortex Breakdown

The effects of the variation of the relative location of vortex breakdown on the crossflow structure are demonstrated in Fig. 6, which shows instantaneous streamline patterns (left column) and contours of constant vorticity (right column). This set of data was obtained for $\phi = -15$ deg, in a crossflow plane located at 90% chord. In each case, the leading-edge vortex on the port side of the delta wing breaks down at the apex, whereas the leading-edge vortex on the starboard side of the wing remains coherent over most of the chord. The schematic in Fig. 6 shows the relative breakdown location for each of the images A through C. Specifically, these three images correspond to cases for which $(x_{vb} - x_L)/c_o$ is equal to 0.3, 0.1, and -0.1 , respectively.

In image A, for which breakdown occurs downstream of the trailing edge on the starboard side, the crossflow topology of the primary vortex is characterized by a set of nested limit cycles, with a stable limit cycle appearing at the outermost edge of the vortex and an unstable limit cycle appearing in the core of the vortex. In image B, the location of vortex breakdown has moved upstream to the trailing edge on the starboard side, and the corresponding streamline topology has changed to an outwardly spiraling (unstable) focus. Finally, in image C, the breakdown occurs over the surface of the delta wing, and the streamline topology on the starboard side is now in the form of an unstable limit cycle. These results clearly show that the instantaneous streamline patterns in the crossflow plane of the leading-edge vortex may exhibit several topological forms and that these classes of topology are related to the self-excited movement of the location of leading-edge vortex breakdown relative to the plane of view. In each image, the streamline topology on the port side of the wing is unstable (outwardly spiraling) in nature, which has been observed previously in a crossflow plane containing fully stalled flow.

The vorticity contours shown in the right column of Fig. 6 exhibit patterns of small-scale, negative vorticity on the port side in each image, indicating a region of stall caused by the onset of vortex breakdown occurring at the apex. In contrast, the starboard side contains relatively concentrated contours of positive vorticity, indicating a more coherent structure of the leading-edge vortex. Comparison of images A, B, and C shows that as the breakdown position moves upstream, the spatial extent of the primary vortex expands slightly and the maximum vorticity level decreases. Also note that, although there are no coherent structures on the port side of these images, there is a definite roll-up of the corresponding streamline pattern, again indicating that consideration of only streamline patterns or vorticity contours may not provide a complete description of the flow structure. Furthermore, whereas the streamline patterns are distinctly different depending on the location of vortex breakdown relative to the FOV, the patterns of contours of constant vorticity reveal no such abrupt change in form.

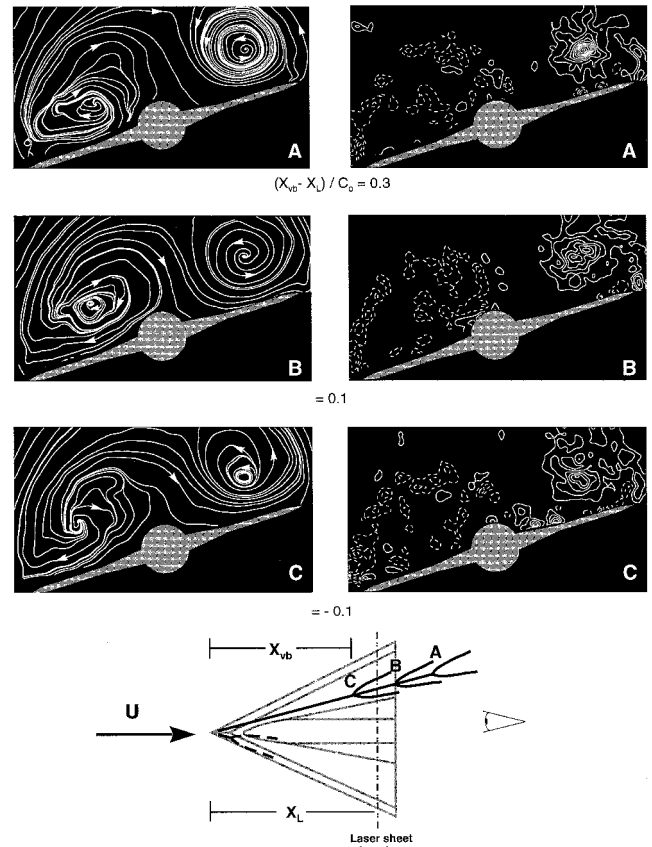


Fig. 6 Instantaneous streamline patterns and vorticity fields at three different instants of time when the onset of breakdown of the starboard vortex is in the immediate vicinity of the plane of observation. $\phi = -15$ deg, $\omega_{min} = \pm 10 \text{ s}^{-1}$, and $\Delta\omega = 10 \text{ s}^{-1}$.

Conclusions

The flow structure in a crossflow plane of a delta wing has been characterized in terms of the instantaneous vorticity and streamline patterns possible immediately after the onset of and within regions of vortex breakdown. It is demonstrated that self-excited excursions of vortex breakdown can give rise to different topological states at a given crossflow plane. In addition, there are situations where the breakdown position may not vary, but the local, instantaneous variations of the vorticity field may be associated with different instantaneous streamline topologies.

Instabilities inherent to the flow past a delta wing are illustrated by fluctuations in the flow patterns for a stationary wing. Often transformations occur independently in either the streamline or vorticity patterns, indicating that both representations are necessary to provide a complete description of the flow structure. In cases where large excursions of the vortex breakdown location occur, corresponding deviations of the instantaneous topologies suggest that traditional, time-averaged topologies may not be meaningful in interpreting the physics of this class of flows. Finally, the sectional streamline patterns as well as the contours of constant vorticity reveal that coupling exists between the opposite leading-edge vortices.

Acknowledgments

Primary support for this project was received from the U.S. Air Force Office of Scientific Research, with supplemental support from the Office of Naval Research and the National Science Foundation.

References

- Tobak, M., and Peake, D. J., "Topology of Three-Dimensional Separated Flows," *Annual Review of Fluid Mechanics*, Vol. 14, 1982,

pp. 1461–1485.

²Perry, A. E., and Chong, M. S., “A Description of Eddying Motions and Flow Patterns Using Critical-Point Concepts,” *Annual Review of Fluid Mechanics*, Vol. 19, 1987, pp. 125–155.

³Visbal, M. R., “Structure of Vortex Breakdown on a Pitching Delta Wing,” AIAA Paper 93-0434, Jan. 1993.

⁴Rockwell, D., “Three-Dimensional Flow Structure on Delta Wings at High Angle of Attack: Experimental Concepts and Issues,” AIAA Paper 93-0550, Jan. 1993.

⁵Magness, C., Robinson, O., and Rockwell, D., “Instantaneous Topology of the Unsteady Leading-Edge Vortex at High Angle of Attack,” *AIAA Journal*, Vol. 31, No. 8, 1993, pp. 1384–1391.

⁶Visbal, M. R., and Gordnier, R. E., “Crossflow Topology of Vortical Flows,” *AIAA Journal*, Vol. 32, No. 5, 1993, pp. 1085–1087.

⁷Hanff, E. S., and Jenkins, S. B., “Large-Amplitude High-Rate Roll Experiments on a Delta Wing and Double Delta Wing,” AIAA Paper 90-0224, Jan. 1990.

⁸Hanff, E. S., and Huang, X. Z., “Roll-Induced Cross-Loads on a Delta Wing at High Incidence,” AIAA Paper 91-3223, Sept. 1991.

⁹Ericsson, L. E., and Hanff, E. S., “Unique High-Alpha Roll Dynamics of a Sharp-Edged 65 Deg Delta Wing,” AIAA Paper 92-0276, Jan. 1992.

¹⁰Ericsson, L. E., and Hanff, E. S., “Further Analysis of High-Rate Rolling Experiments of a 65 Deg Delta Wing,” AIAA Paper 93-0620, Jan. 1993.

¹¹Jenkins, J. E., Myatt, J. H., and Hanff, E. S., “Body-Axis Rolling Motion Critical States of a 65-Degree Delta Wing,” AIAA Paper 93-0621, Jan. 1993.

¹²Cipolla, K., Liakopoulos, A., and Rockwell, D., “Quantitative Imaging in Proper Orthogonal Decomposition of Flow Past a Delta Wing,” *AIAA Journal* (submitted for publication).

¹³Cipolla, K., “Structure of the Flow Past a Delta Wing with Variations in Roll Angle,” Ph.D. Dissertation, Lehigh Univ., Bethlehem, PA, June 1996.

¹⁴Gursul, I., and Yang, H., “On Fluctuations of Vortex Breakdown Location,” *Physics of Fluids*, Vol. 7, No. 1, 1995, pp. 229–231.

¹⁵Rockwell, D., Magness, C., Towfighi, J., Akin, O., and Corcoran, T., “High Image-Density Particle Image Velocimetry Using Laser Scanning Techniques,” *Experiments in Fluids*, Vol. 14, 1993, pp. 181–192.

¹⁶Seke, E., “PIV3” Interrogation Software, Fluid Mechanics Lab., Lehigh Univ., Bethlehem, PA, 1993.

¹⁷Hornung, H., and Perry, A. E., “Some Aspects of Three-Dimensional Separation, Part I: Streamsurface Bifurcations,” *Zeitschrift für Flugwissenschaften und Weltraumforschung*, Vol. 8, March 1984, pp. 77–87.

¹⁸Vorobieff, P. V., “Multiple-Actuator Control of Vortex Breakdown on a Maneuvering Delta Wing and Related Issues of Flow Analysis and Topology,” Ph.D. Dissertation, Lehigh Univ., Bethlehem, PA, June 1996.